Supplementary Materials for

Rational Design and Size Regulation of Unimolecular Nanoparticles for Constructing Diverse Superlattices in Soft Matter

Huanyu Lei, Xing-Han Li, Han Hao, Yuchu Liu, Qing-Yun Guo*, Mingjun Huang[1]*

*Corresponding author.
Email: qg6@uakron.edu (Q.-Y. G.), huangmj25@scut.edu.cn (M.H.)

This PDF file includes:

1. Materials and Characterizations

1.1 Chemicals and solvents

Tri-Silanol-Isooctyl POSS was purchased from Hybrid Plastics and used as received; gel permeation chromatography (GPC) was performed by Bio-BeadsTM S-X Resin; other chemicals and solvents were used as received from Sigma-Aldrich, Acros Organic, or Fisher Scientific.

1.2 Characterization

Giant molecular monomer samples. All pure giant molecules were transferred into separate vials and dried under vacuum before further operation.

Giant molecular (GM) blends. Equal mass (30 mg) of each giant molecule was separately dissolved in 3.0 mL of methylene chloride, different volumes of solution (for example 100 μL, 200 μL...500 μL) were taken and mixed to afford target compositions. By mixing two different solutions, the blends were prepared. Then evaporation the methylene chloride, re-dissolved in benzene (0.4 mL) and freeze-dried to erase the "thermal history" of the samples before further thermal treatment, affording sticky white solid powder.

Bulk sample for small-angle X-ray diffraction (SAXD). A small piece of blended sample was taken and placed into an aluminum ring and sealed by Kapton tape. A Mettler Toledo FPHT hot stage was used for sample annealing. All thermal annealing processes were performed under the Argon atmosphere. Blends of different compositions were annealed at different target temperatures for at different times; for each composition, at least three pieces of samples were annealed at the same time to confirm reproducibility.

TEM sample preparation. TEM sample preparation. The samples for TEM experiments were prepared by dropping 5 μL sample solution (1 mg/mL in tetrahydrofuran) onto surface of water. After the solvent evaporation, the sample reflects blue-violet light, suggesting that the thickness is around a hundred nanometers. Then transfer the thin film to a carbon-coated copper grid. After the remaining water has completely evaporated, the copper grids were annealed as the method described above, after annealing, sample were further stained by RuO_4 staining method for 10-15 min.

Nuclear magnetic resonance (NMR) spectroscopy. ^{1}H and ^{13}C experiments were measured on a Varian Mercury 500 M NMR and 125 M NMR spectrometer. ^{1}H NMR spectra were referenced to the

residual solvent peak in $CDCl_3$ at δ 7.26 ppm and in DMSO-d_6 at δ 2.50 ppm, and ^{13}C NMR spectra were referenced to the residual solvent peak in $CDCl_3$ at δ 77.00 ppm.

Gel permeation chromatography (GPC). GPC analyses were performed on a Waters 150-C Plus instrument equipped with three HRStyragel columns [100 Å, mixed bed (50/500/103/104 Å), mixed bed (103, 104, 106 Å)], and a triple detector system. The three detectors included a differential viscometer (Viscotek 100), a laser light scattering detector (Wyatt Technology, DAWN EOS, λ = 670 nm), and a differential refractometer (Waters 410). THF was used as the eluent with a flow rate of 1.0 mL/min at room temperature. Data processing was accomplished using the build-in software on the workstation.

Mass Spectroscopy (MS). Matrix-assisted Laser Desorption/Ionization Time-of-Flight (MALDI-TOF) MS of the samples were collected on a Bruker Ultra flex-III MALDI-TOF/TOF mass spectrometer equipped with a Nd laser (355 nm). Trans-2[3-(4ter-butylphenyl)-2-methyl-2proenylidene] malononitrile (DCTB) was used as matrix. And sodium trifluoroacetate was used as the cationizing salt for all samples.

Thermogravimetric analysis (TGA). The non-isothermal decomposition experiments were carried out in a thermogravimetric analysis instrument (Model Q500, TA Instruments) in air. For each run of the experiments, initial mass of the samples used was 5 mg, scanning within the temperature range of 30 to 600 °C with a heating rate of 10 °C/min.

Differential scanning calorimetric experiments (DSC). were carried out in DSC 2500 by TA Instruments. An initial mass of the samples used was 3-5 mg, scanning within the temperature range of -40 to 250 °C with a heating rate of 10 °C/min.

Density measurements. The prepared sample was soaked with water in a vial. Then, saturated potassium iodide aqueous solution was added dropwise into the vial until the sample was suspended in the solution for 30 mins. At this point, the density of the sample is identical with the solution. The solution was then transferred into a volumetric flask. The density of the solution was calculated by weight divided by volume. The experimentally measured density of these phases formed by the giant molecules are about ρ = 1.07 (g/cm^3), and that of dendron-like giant molecule **H-PhO$_3$** is ρ = 1.14 (g/cm^3)

Small-angle x-ray diffraction (SAXD). The X-ray diffraction data were recorded at beamline BL16B1 of the Shanghai Synchrotron Radiation Facility (SSRF) at a wavelength of 1.2398 Å. Beamline BL16B1 is based on bending magnet and a Si (111) double crystal monochromator was employed to

monochromatize the beam. The spot size is 0.39 * 0.48 mm^2, and Pilatus 200K-A detector was used for data collection. Silver(I) behenate standard sample was determined for d-spacing calibration. The 1D circular integrations of 2D SAXS patterns were performed by Igor Pro 6.37 (with Nika 2D SAS macros) software package. Besides, some SAXD experiments were performed on a Xeuss 2.0 instrument equipped with a two-dimensional Pilatus 3R 1M detector and a 300 W MetalJet D2 liquid metal light source. The recording time for each sample was 15 mins. The data analysis was done with Foxtrot software.

Transmission electron microscopy (TEM). A JEM 1400 Plus TEM with an accelerating voltage of 120 kV was utilized to record the bright-field (BF) images of thin sections of different samples. BF-TEM images were collected on a digital CCD camera and processed with the accessory digital imaging system.

Molecular modeling. The molecular and mesoatomic models were constructed and optimized using the Material Studio simulation package. The Condensed-phase Optimized Molecular Potential for Atomistic Simulation Studies (COMPASS II) force field was used to perform the geometry optimization.

1.3 Analysis of number of Giant molecules incorporated in each mesoatom.

$$\frac{4}{3}\pi R_m^3 = \frac{V_{unit\ cell}}{N_{lattice}} \quad \rightarrow \quad R_m = \sqrt[3]{\frac{3 \times a_{lattice}^3}{4\pi \times N_{lattice}}}$$

$$V_{motif} \times \rho = n_{GM} \times \frac{M_{GM}}{N_A} \quad \rightarrow \quad N = \frac{4\pi \times R_m^3 \times \rho \times N_A}{3 \times M_{GM}}$$

R_m: $effective\ radius\ of\ \ spherical\ motifs$ $V_{unit\ cell}$: $volume\ of\ unit\ cell$

$N_{lattice}$: $number\ of\ mesoatoms\ per\ lattice$ $a_{lattice}$: $cubic\ lattice\ parameter$

V_{motif}: $volum\ of\ motif$ ρ: $density\ of\ sample$

N: $number\ of\ giant\ molecules\ per\ moitf$ M_{GM}: $molecular\ weight\ of\ giant\ molecule$

(1) E.g., FK A15 superlattice of βCD-ii:

$a_{A15} = 7.34\ nm, N_{A15} = 8$

$M_{\beta CD-ii} = 31890\ g \cdot mol^{-1}, N_A = 6.02 \times 10^{23}\ mol^{-1}$

$$R_m = \sqrt[3]{\frac{3 \times (7.34\ nm)^3}{4\pi \times 8}} = 2.28\ nm$$

$$N = \frac{4\pi \times (2.28\ nm)^3 \times 1.07 g \cdot cm^{-3} \times 6.02 \times 10^{23}\ mol^{-1}}{3 \times 31890\ g \cdot mol^{-1}} = 1.0$$

(2) E.g., BCC superlattice of βCD-iv:

$a_{BCC} = 5.76\ nm, N_{BCC} = 2$
$M_{\beta CD-iv} = 62833\ g \cdot mol^{-1}$, $N_A = 6.02 \times 10^{23}\ mol^{-1}$

$$R_m = \sqrt[3]{\frac{3 \times (5.76\ nm)^3}{4\pi \times 2}} = 2.84\ nm$$

$$N = \frac{4\pi \times (2.84\ nm)^3 \times 1.07 g \cdot cm^{-3} \times 6.02 \times 10^{23}\ mol^{-1}}{3 \times 62833\ g \cdot mol^{-1}} = 1.0$$

2. Synthesis parts

The compounds were all prepared in a "molecular Lego" approach. The β-cyclodextrin core (βCD-21yne) is prepared according to our previous work[1]. The synthesis routes of OPOSS ligands were in **Fig. S1**. Some of them are provided in previous publication[2, 3]. Finally, the "core" part and OPOSS ligands were connected through a copper-catalyzed azide-alkyne [3 + 2] cycloaddition (CuAAC) "click" chemistry, which could offer all the finally 4 kinds of giant molecules with the yield above 80%.

Example of OPOSSS ligands ii:

Firstly, OPOSS with NH_2 groups (1.27 g, 1 mmol) was dissolved in DCM (100 mL) and reacted with benzyl azide benzoic acid (212 mg, 1.2 mmol, 1.2 eq.) using EDC/HOBT catalytic system for amido synthesis. The mixture was stirred at 0 ℃ for 24 h. Then the solvent was removed by rotary evaporation and the resulting solid was purified by chromatography (PE:EA=4:1 as eluent) to provide the product OPOSSS ligands ii as colourless sticky liquid. Other ligands with amide groups are using similar system and EDC/DMAP catalytic system for easter synthesis.

Example of Final compounds:

The core βCD-21yne (20 mg, 0.010 mmol) and OPOSS ligands ii (930 mg, 0.652 mmol, 63 eq.) was dissolved in 10 mL toluene in dry box. CuBr (0.1 mmol, 15 mg) and PMDETA (200 mg, 250 μL) was added into solution in sequence. The mixture was stirred at room temperature overnight. The reaction was stopped by open to atmosphere, the copper salt was removed by silica gel chromatography (DCM/MeOH as eluent). The solvent was removed under vacuum and the crude product was further purified by size exclusion chromatography afford the pure compounds.

The NMR results are as follows:

Ligand i. OPOSS-a_6-N_3

^{1}H NMR (400 MHz, $CDCl_3$) δ 6.27 (s, 1H), 3.98 (s, 2H), 3.28 (m, 2H), 1.82 (s, 7H), 1.63 (m, 2H) 1.32-1.10 (d, 14H), 1.07-0.96 (m, 21H), 0.96-0.82 (m, 63H), 0.76-0.49 (m, 18H).

Ligand ii. OPOSS-a_5-Ph-a_1-N_3

^{1}H NMR (400 MHz, $CDCl_3$) δ 7.74(d, 2H), 7.38 (d, 2H), 6.04 (s, 1H),4.39 (s, 2H), 3.44 (t, 2H), 1.80 (s, 7H), 1.71 (m, 2H) 1.32-1.10 (d, 14H), 1.07-0.96 (m, 21H), 0.96-0.82 (m, 63H), 0.81-0.49 (m, 18H).

Ligand iii. OPOSS-a_7-Ph-a_1-N_3

^{1}H NMR (400 MHz, $CDCl_3$) δ 8.05(d, 2H), 7.40 (d, 2H), 4.42 (t, 4H), 2.88 (t, 2H), 2.71 (d, 2H), 1.82 (s, 7H), 1.32-1.10 (d, 14H), 1.07-0.96 (m, 21H), 0.96-0.82 (m, 63H), 0.81-0.49 (m, 16H).

Ligand iv. (OPOSS-a_7)$_2$-C-Ph-a_{3+1}-N_3

^{1}H NMR (400 MHz, $CDCl_3$) δ 8.02 (dd,2H), 7.41 (dd,2H), 4.42 (s, 2H), 4.28 (s, 2H), 4.17 (s, 4H), 3.23 (s, 4H), 2.74 (t, 4H), 1.82 (s, 14H), 1.43 (s, 3H), 1.32-1.10 (d, 28H), 1.07-0.96 (m, 42H+3H), 0.96-0.82 (m, 126H), 0.81-0.49 (m, 32H).

βCD type of giant molecules

βCD-i

^{1}H NMR (400 MHz, $CDCl_3$) δ 8.20-7.80 (t), 5.24 (-CH_2-COO-, m), 4.28 (s, -COO-CH_2-), 2.80-2.60 (s,-CH_2-S-CH_2-), 1.82 (s, H of OPOSS), 1.32-1.10 (d), 1.07-0.96 (m), 0.96-0.82 (m), 0.80-0.49 (m). **^{13}C NMR** (500 MHz, $CDCl_3$) δ 77.35, 77.10, 76.84, 59.63, 54.04, 41.50, 31.25, 30.28, 25.81, 25.05, 20.96, 1.11.

βCD-ii

^{1}H NMR (400 MHz, $CDCl_3$) δ 7.68 (s, phenyl H), 3.39 (s, -CONH-CH2-), 1.82 (s, H of OPOSS), 1.32-1.10 (d), 1.07-0.96 (m), 0.96-0.82 (m), 0.81-0.49 (m). **^{13}C NMR** (500 MHz, $CDCl_3$) δ 77.10, 60.05, 53.93, 31.24, 30.25, 25.76, 25.04, 23.66, 1.11.

βCD-iii

^{1}H NMR (400 MHz, $CDCl_3$) δ 7.93-7.34 (m, phenyl H), 4.39 (s, -COO-CH_2-), 2.83-2.66 (s, -CH_2-S-CH_2-), 1.82 (s, H of OPOSS), 1.32-1.10 (d), 1.07-0.96 (m), 0.96-0.82 (m), 0.81-0.49 (m). **^{13}C NMR** (500 MHz, $CDCl_3$) δ 76.84, 56.39, 31.24, 30.26, 25.78, 25.04, 1.11.

βCD-iv

^{1}H NMR (400 MHz, $CDCl_3$) δ 7.92 (s, phenyl H), 4.24-4.12 (s, -CH_2-$CHCH_3$-CH_2-), 3.22 (s, -OOC-CH_2-S-), 2.73 (s, -S-CH_2-), 1.82 (s, H of OPOSS), 1.32-1.10 (d), 1.07-0.96 (m), 0.96-0.82 (m), 0.81-0.49 (m). **^{13}C NMR** (500 MHz, $CDCl_3$) δ 77.09, 51.44, 31.24, 30.25, 27.87, 26.42, 25.04, 23.69, 0.65.

3. **Supplementary Figures**

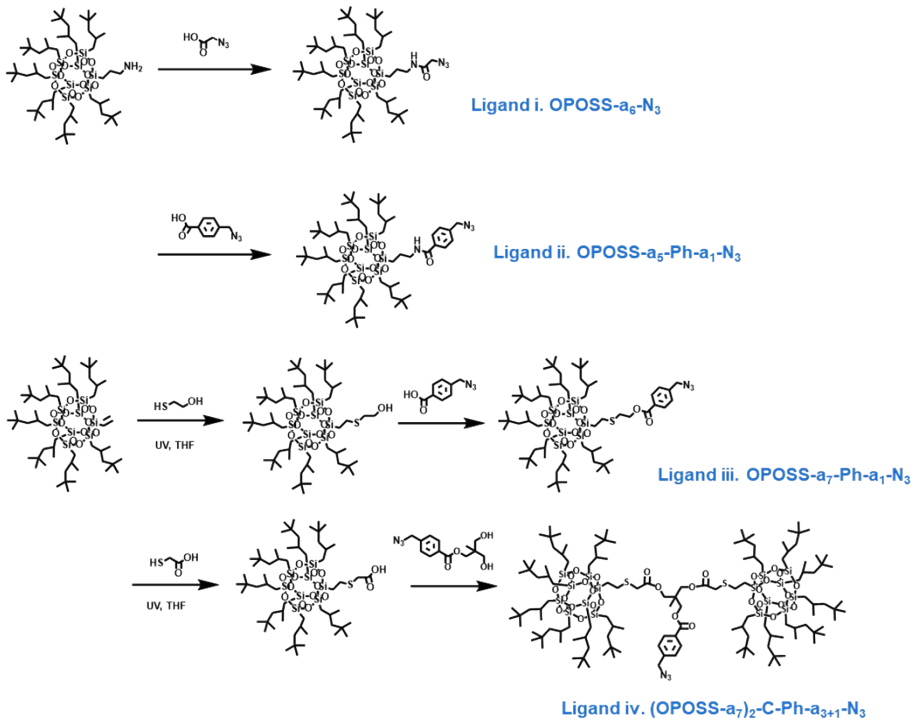

Fig. S1 General synthesis route of ligands OPOSS.

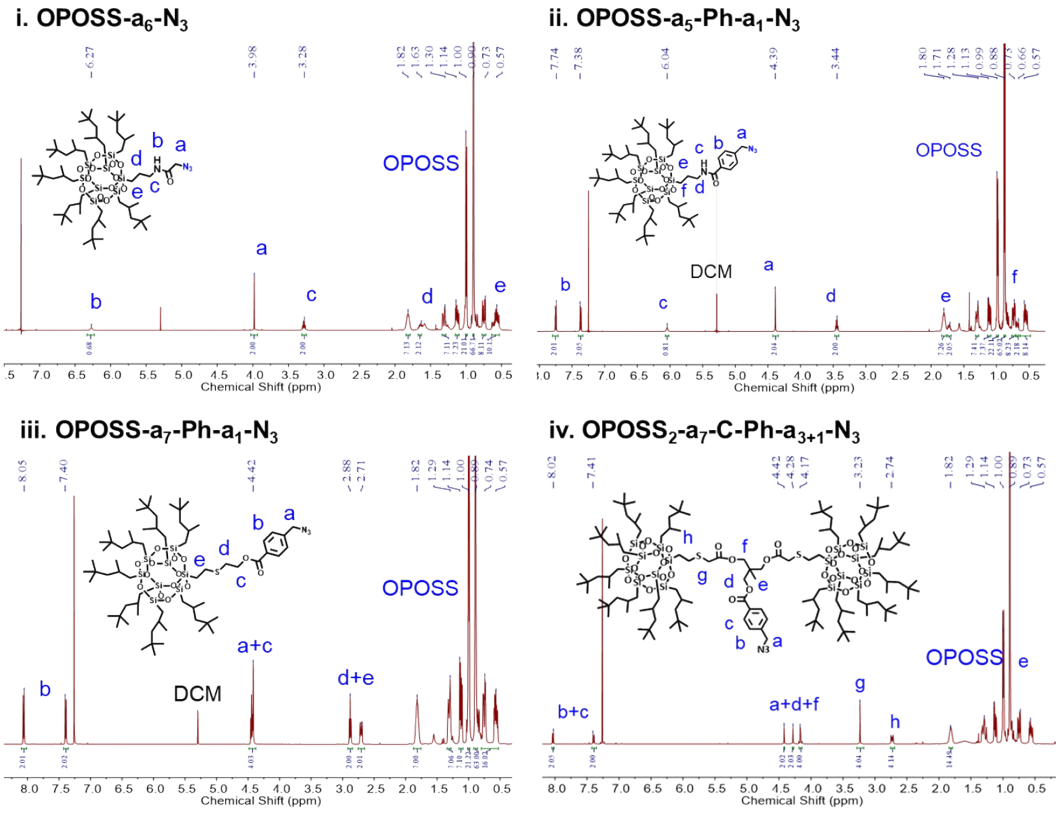

Fig. S2 ^{1}H NMR results of OPOSS ligands **i** to **iv**.

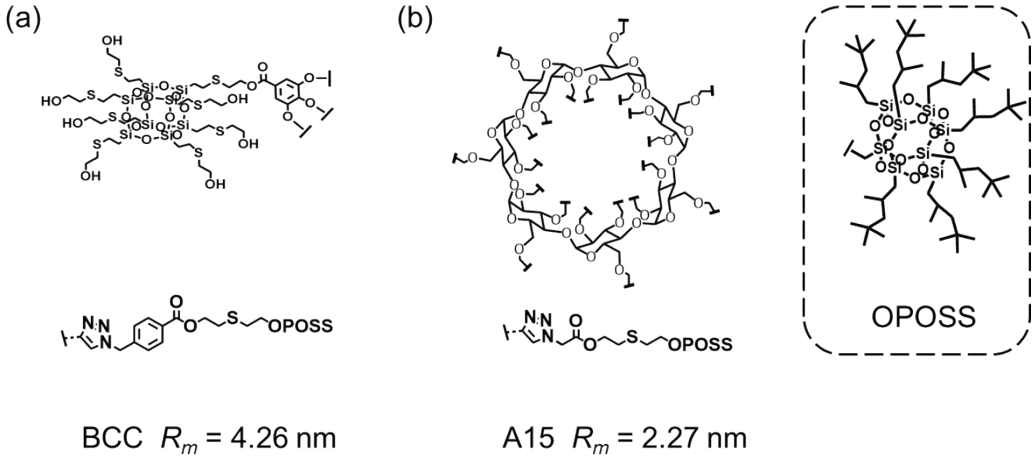

Fig. S3 Chemical structures of giant molecules published before (a) **H-PhO$_3$**, and (b) **βCD-O$_{21}$**.

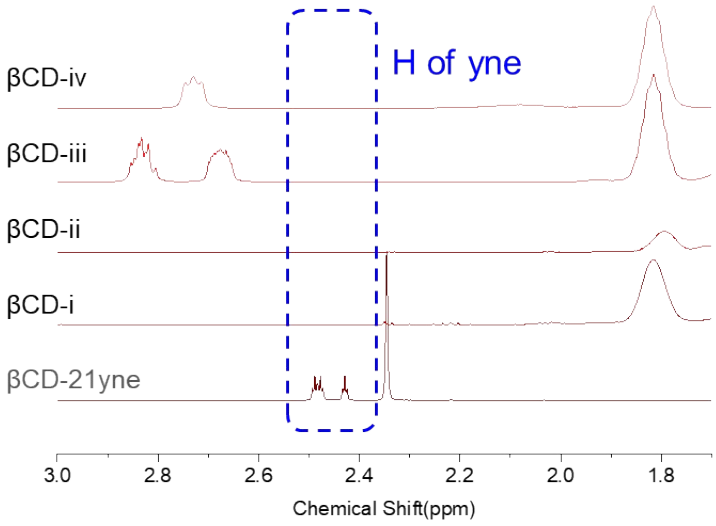

Fig. S4 Magnified ^{1}H NMR results of **βCD-i** to **βCD-iv**.

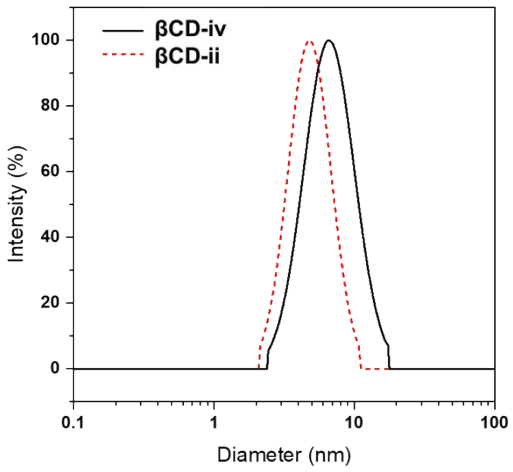

Fig. S5 DLS results of **βCD-ii** and **βCD-iv**.

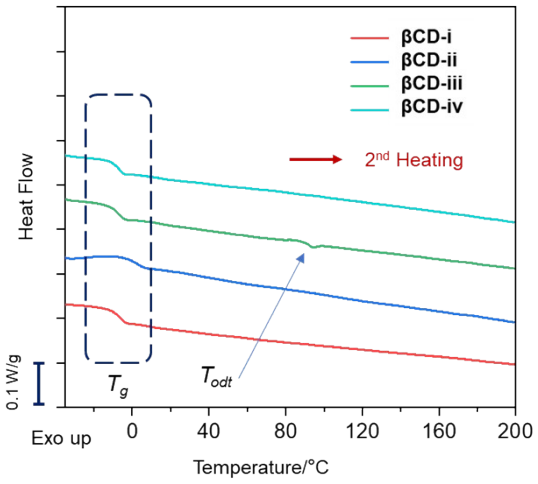

Fig. S6 DSC curves of **βCD** type of giant molecules.

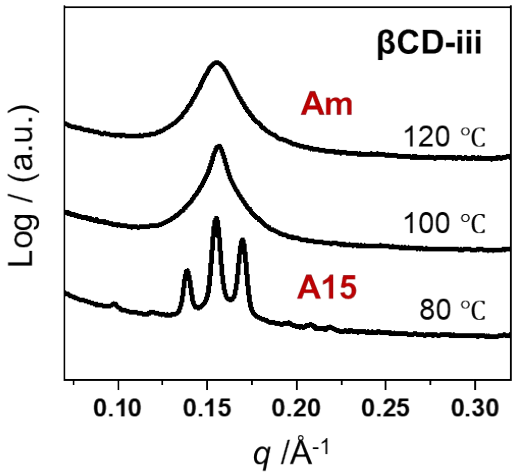

Fig. S7 SAXD results of giant molecule **βCD-iii** annealed at different temperatures.

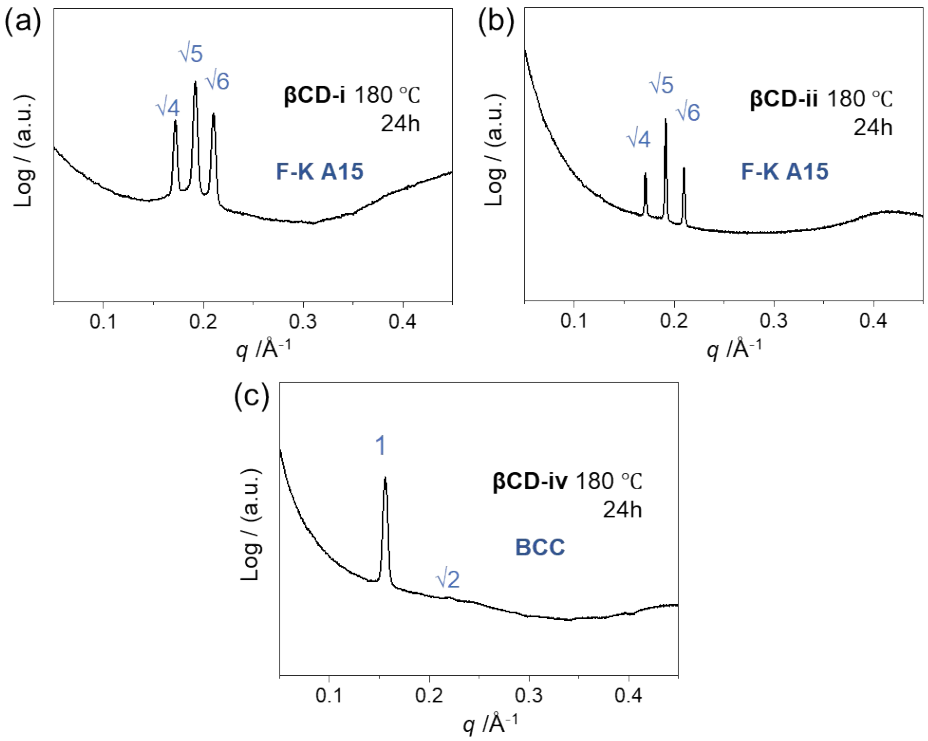

Fig. S8 SAXD results of βCD-type UMNPs annealed at higher temperatures (180°C).

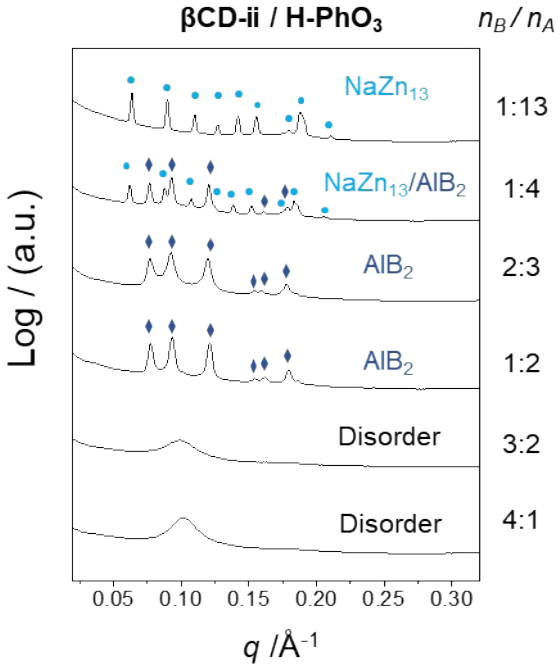

Fig. S9 SAXD results of **βCD-ii/H-PhO$_3$** binary blends

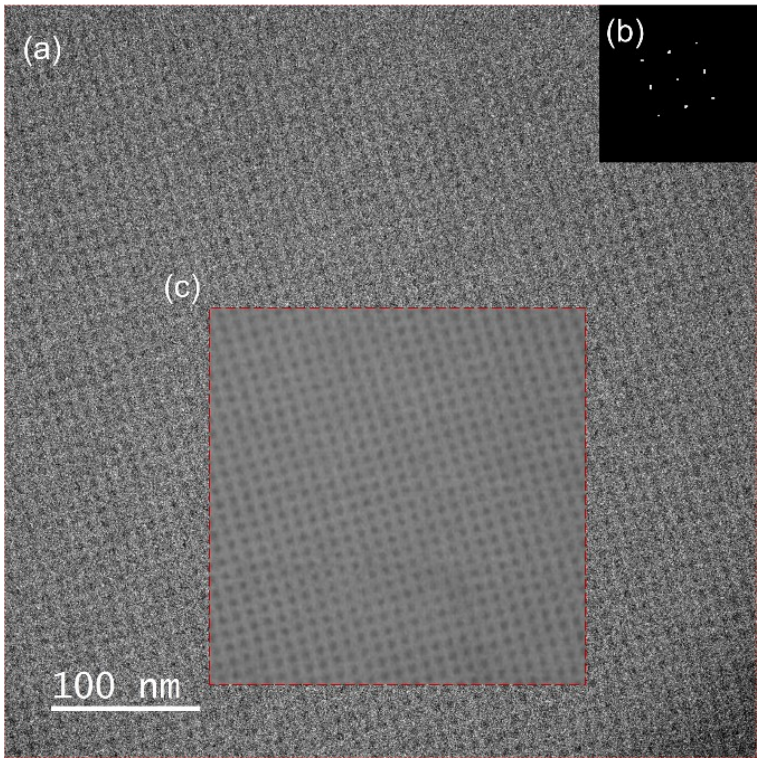

Fig. S10 TEM characterization of **βCD-ii/H-PhO$_3$** corresponding view from [100] direction of $NaZn_{13}$-type superlattice (a) BFTEM image, (b) FFT pattern, (c) FFT-filtered BFTEM image

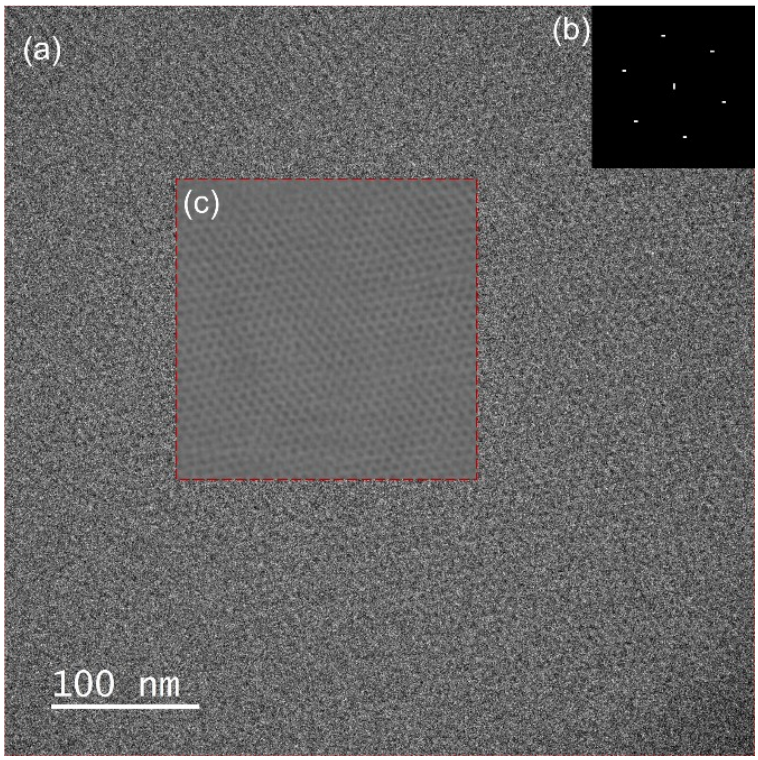

Fig. S11 TEM characterization of **βCD-ii/H-PhO$_3$** corresponding view from [001] direction of AlB_2-type superlattice (a) BFTEM image, (b) FFT pattern, (c) FFT filtered BFTEM image

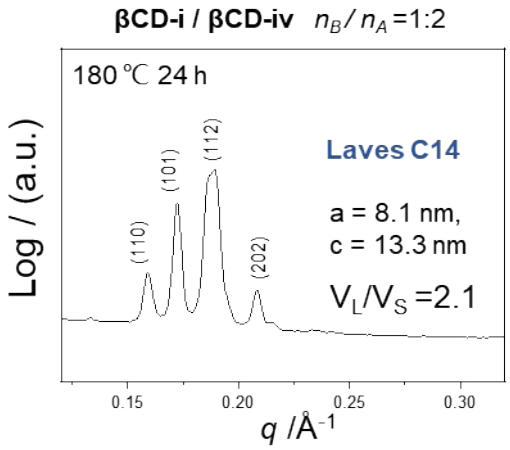

Fig. S12 SAXD results of **βCD-i/βCD-iv** binary blends

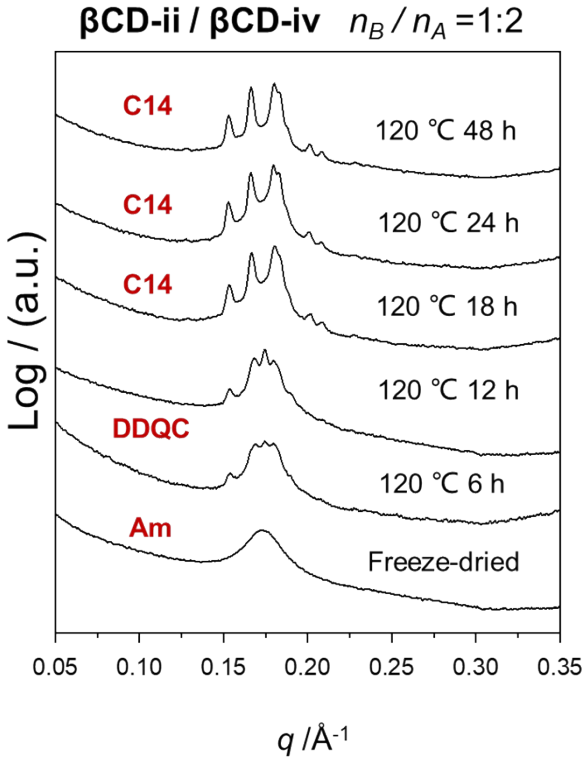

Fig. S13 SAXD results of binary **βCD-ii/βCD-iv** blends annealing at different times**.**

4. Supplementary Tables

Table S1. GPC results of different giant molecules

No.	$M_{w.\ cal}$	$M_{w.\ GPC}$	PDI	Linker length /Å*
βCD-i	28941	5.87 k	*1.005*	10.7
βCD-ii	31890	6.64 k	*1.004*	14.9
βCD-iii	32878	7.65 k	*1.003*	18.3
βCD-iv	62833	11.5 k	*1.005*	24.3

*Calculated by DFT/B3LYP/6-311gd+.

Table S2. Thermal properties of different giant shape amphiphiles

Sample	$T_{95\%}$ / °C	T_g / °C	T_{ODT} / °C	ΔH / kJ·mol^{-1}
βCD-i	337	-8.9	/	/
βCD-ii	380	-0.3	/	/
βCD-iii	357	-8.9	87.4	12.8
βCD-iv	368	-8.2	/	/

Table S3. Summarized characterization data of binary blends

Constitution	R ratio	V_L/V_S ratio	BNSLs	Lattice parameters/nm
βCD-ii / iv	2.28 / 2.84	1.9	Laves C14	$8.2^2\times13.5$
βCD-i / iv	2.20 / 2.84	2.2	Laves C14	$8.1^2\times13.3$
βCD-ii / H-PhO$_3$	2.28 / 4.26	6.5	$NaZn_{13}$	19.8
			AlB_2	$7.8^2\times8.1$

Table S4. Observed and calculated peak positions for the $NaZn_{13}$ superlattice in **βCD-ii / H-PhO$_3$**, n_B/n_A = 1:13, at 120 ºC for 24h. Peak positions were calculated using $Fm\bar{3}c$ space group symmetry with lattice parameters a = 19.8 nm.

Miller Indices (***hkl***)	q_{obs} (Å^{-1})	q_{calc} (Å^{-1})	%Residual ($\Delta q/q_{calc} \times 100$)
(200)	0.0636	0.0635	-0.16
(220)	0.0901	0.0897	-0.45
(222)	0.1101	0.1099	-0.18
(400)	0.1269	0.1269	0.00
(420)	0.1421	0.1419	-0.14
(224)	0.1556	0.1554	-0.13
(440)	0.1794	0.1795	0.06
(531)	0.1881	0.1877	-0.21
(622)	0.2102	0.2105	0.14

Table S5. Observed and calculated peak positions for the AlB_2 superlattice in **βCD-ii / H-PhO$_3$**, n_B/n_A = 1:2 at 100 ºC for 24h. Peak positions were calculated using *P6/mmm* space group symmetry with lattice parameters a = 7.8 nm, c = 8.1 nm

Miller Indices (***hkl***)	q_{obs} (Å^{-1})	q_{calc} (Å^{-1})	%Residual ($\Delta q/q_{calc} \times 100$)
(001)	0.0771	0.0773	0.26
(100)	0.0933	0.0933	0.00
(101)	0.1209	0.1211	0.17
(002)	0.1545	0.1546	0.06
(110)	0.1615	0.1615	0.00
(111)	0.1794	0.1791	-0.17
(200)	0.1864	0.1865	0.05

Table S6. Observed peak positions for the Laves C14 superlattice formed upon annealing **βCD-ii / iv**, at 180 ºC for 24h. Peak positions were calculated using *P6₃/mmc* space group symmetry with lattice parameters a = 8.2 nm, c =13.3 nm for Laves C14.

Miller Indices (***hkl***)	q_{obs} (Å^{-1})	q_{calc} (Å^{-1})	%Residual ($\Delta q/q_{calc} \times 100$)
(102)	0.1299	0.1295	-0.31
（110）	0.154	0.1538	-0.13
（103）	0.1671	0.1669	-0.12
（112）	0.1801	0.1804	0.17
(201)	0.1837	0.1837	0.00
(004)	0.1882	0.1884	0.11
(202)	0.2013	0.201	-0.15
(104)	0.2083	0.2083	0.00

5.References

[1] Lei H.; Liu Y.; Liu T., et al. Unimolecular Nanoparticles toward More Precise Regulations of Self-Assembled Superlattices in Soft Matter [J]. Angew. Chem., Int. Ed., 2022, 61, e202203433.

[2] Liu Y.; Liu G.; Zhang W., et al. Cooperative Soft-Cluster Glass in Giant Molecular Clusters [J]. Macromolecules, 2019, 52, 4341-4348.

[3] Lei H.; Li X.; Liu Y., et al. Diverse Superlattices Constructed via Perylene Bisimide Type of Giant Shape Amphiphiles: Assisted with Unimolecular Nanoparticles [J]. Thermochim. Acta., 2023, 719, 179411.

6.Author contributions

Conceptualization: H.L. Y. L.;
Methodology: H.L., X-H.L., H.H.,Y. L.;
Formal Analysis: H.L., X-H.L.;
Writing - original draft: H.L.;
Writing - review & editing: H.L., Q-Y.G, M. H.